Tensile behaviour of nonwoven structures: comparison with experimental results

Amit Rawal · Apurv Priyadarshi · Narender Kumar · Stepan V. Lomov · Ignaas Verpoest

Abstract Nonwoven structures have been recently explored for numerous novel applications ranging from composites to scaffolds. The tensile property of nonwovens is a pre-requisite and indeed, one of the main parameters to determine their performance for such applications. In the first part, a modified micromechanical model describing the tensile behaviour of thermally bonded nonwovens was proposed by incorporating the effect of fibre re-orientation during the deformation (Rawal et al., J Mater Sci 45:2274, 2010). In this study, an attempt has been made to compare the theoretical and experimental stress–strain curves of thermally bonded and spunbonded nonwoven structures. These theoretical findings have been obtained from the most popular analytical tensile models of nonwovens available in the literature in addition to our modified tensile model. Poisson's ratio has also been determined experimentally in order to predict the stress–strain behaviour of nonwoven, and its relationship with longitudinal strain has clearly distinguished between the randomly and preferentially orientated types of structures. In thermally bonded nonwovens, the tensile strength in various test directions is computed through pull-out stress and a comparison is made with the experimental results.

A. Rawal (✉) · A. Priyadarshi · N. Kumar
Department of Textile Technology, Indian Institute
of Technology Delhi, Hauz Khas, New Delhi, India
e-mail: arawal@textile.iitd.ac.in; amitrawal77@hotmail.com

S. V. Lomov · I. Verpoest
Department of Metallurgy and Material Engineering,
Katholieke Universiteit Leuven, Kasteelpark Arenberg, 44,
3001 Leuven, Belgium

Introduction

Nonwovens are complex anisotropic fibrous assemblies that consist of fibres aligned in preferential or random directions and simultaneously, bonded by thermal, chemical or mechanical means. Recently, these structures have been explored for numerous novel applications ranging from composites to scaffolds [1–3]. Nevertheless, all these applications have a common pre-requisite, i.e. the structures should not disintegrate into individual fibres/filaments on applying the load. Therefore, the tensile property of nonwovens is of paramount importance and indeed, one of the main parameters to determine their performance for such application. It should be noted that each type of nonwoven has distinct structural characteristics in terms of fibres and bond behaviour that needs to be accounted for accurate prediction of tensile deformation.

In general, the two most popular theories that have been generally used for predicting the tensile deformations of nonwoven structures are orthotropic and fibre network theories [4–8]. The orthotropic theory is based on *classical lamination* theory whereby a nonwoven has been assumed as a layered structure defined as *laminate* and each layer is known to be *lamina*. On the other hand, fibre network theory is based on incremental deformation principle whereby the nonwoven is divided into numerous *unit cells* experiencing same strain as that of a fabric and the average strain developed in each fibre can be considered as equivalent to the strain experienced by the fibre which is bonded at the boundaries of unit cell. One of the limitations of these theories is that the number of bonds formed between fibres, which are responsible for the transfer of load have not been accounted. Nevertheless, the number of fibre–fibre contacts or bonds between the fibres in a given volume has been deduced by various researchers [9–13].

In addition to analytical approaches, more recently a series of articles have been reported to predict the stress–strain properties of thermally bonded nonwovens based on finite element techniques [14–18]. Some of these researchers have also noted that finite element analysis technique has serious challenges to model nonwoven structures due to their inherent discontinuous structural characteristics [16].

In our previous article, various theories and mathematical models have been critically reviewed to predict the stress–strain behaviour of thermally bonded nonwoven structures [19]. Our article has also described the theoretical basis to model the stress–strain behaviour of thermally bonded nonwoven structure by considering the effect of fibre re-orientation during the tensile deformation of a nonwoven structure. The failure criterion of thermally bonded nonwovens has also been analysed using pull-out behaviour of fibres in the system [20]. In this article, the main objective is to make a comparison between the theoretical and experimental stress–strain curves. These theoretical results have been obtained from the most popular analytical models of stress–strain behaviour of nonwovens available in the literature in addition to our modified tensile model [6, 7, 19]. The tensile strength of thermally bonded nonwovens has also been predicted and compared with the experimental findings. Moreover, the initial tensile behaviour of spunbonded nonwoven has also been investigated specifically in the machine direction.

The organisation of this article is as follows: "Theoretical background" section describes briefly the most popular mathematical models available in the literature in addition to the summary of our modified tensile model, incorporating the effect of fibre re-orientation. "Experimental" section presents the experimental work that has been carried out to validate the tensile response of nonwoven structures. Various parameters including shear strain, fibre orientation distribution, Poisson's ratio, fabric physical parameters (mass per unit area, thickness), fibre diameter, fibre- and fabric stress–strain curves have been determined experimentally. In "Results and discussion" section, a comparison is made between the theoretical and experimental stress–strain curves of nonwoven structures. Furthermore, the tensile strength of thermally bonded nonwovens has been determined experimentally and theoretically. A relationship between Poisson's ratio and longitudinal strain is also been analysed, and finally, conclusions are given in "Conclusions" section.

Theoretical background

The two most popular analytical models for predicting the stress–strain behaviour of nonwoven structures are briefly discussed below [6, 7]. In addition, our modified model for predicting the tensile behaviour of nonwovens would also be summarised [19]. In these models, it is assumed that the fibre shape and diameter are invariably constant.

Hearle and Stevenson's tensile model of nonwoven structures [6]

Hearle and Stevenson's tensile model [6] was based on fibre network theory, and the pre-requisite for using the above theory was that fibre stress–strain and fibre orientation distribution need to be known [4]. In general, the fibre network theory assumed that the nonwoven structure is divided into numerous *unit cells* that are large enough to eliminate any local structural variations [4]. These unit cells experience the same strain as that of a fabric, and the average strain developed in each fibre can be considered as equivalent to the strain experienced by the fibre which is bonded at the boundaries of unit cell. Moreover, the bonds were considered inextensible and have higher strength than the constituent fibres. The fibre segment between bonds was also assumed to be straight, but later, fibre curl was introduced by Hearle and Stevenson [6].

As mentioned earlier, the fibre stress–strain behaviour is required for applying the fibre network theory. In general, it is well known that the following constitutive model holds for fibre in tension.

$$\sigma^f = f(\varepsilon_f) \tag{1}$$

where σ^f and ε_f are fibre stress and strain, respectively.

Subsequently, the fabric stress in any given direction can be easily calculated by considering a line of unit length drawn across the fabric and contribution of noninteracting fibres crossing this line is computed. Assuming the fibre oriented at an angle to be φ and the relative frequency of fibres in a defined angular interval be $\chi(\varphi)$, the relative frequency of fibres intersecting a line of unit length is $\chi(\varphi) \cos \varphi$. Furthermore, the component of fibre stress in the test direction will be $\sigma^f \cos \varphi$. Therefore, the fabric stress is calculated by considering the product of component of fibre stresses along with their respective relative frequencies. Assuming the test direction to be α and the fibre orientation angle with respect to test direction (α) to be β_i ($= \varphi - \alpha$).

$$T(\alpha) = \sum_{i=1}^{n} (\sigma^f \cos \beta_i)\{\chi(\beta_i) \cos \beta_i\} \tag{2}$$

where $T(\alpha)$ is the fabric stress in a given test direction (α) and $\chi(\beta_i)$ be a frequency of ith bin of a histogram, representing the distribution as a function of the measured or initial fibre orientation angle (β_i).

The relationship between fibre and fabric strains has also been formulated such that lateral contraction of fabric occurs on applying the longitudinal strain, as shown below.

$$\varepsilon_f = \left(\cos^2 \beta_i (1 + \bar{\varepsilon})^2 + (1 - \bar{\varepsilon}v)^2 \sin^2 \beta_i \right)^{1/2} - 1 \qquad (3)$$

where ε_f is the fibre strain, v is the Poisson's ratio of the fabric in various test directions, and $\bar{\varepsilon}$ is the average fabric strain.

Therefore, the stress–strain of a nonwoven fabric can be obtained by combining the Eqs. 1–3.

Bais-Singh and Goswami's tensile model of nonwoven structures [7]

This model is based on classical *lamination* theory in which the nonwoven (*laminate*) consists of predefined number of layers (*lamina*) of fibres oriented in certain directions, as shown in Fig. 1. Here, the nonwoven is also regarded as assembly of unit cells, and they are large enough to consider defined number of bonds avoiding any local variation in strain levels. It is also assumed that each layer has similar fibre orientation distribution and they are bonded together with each other. Using the elementary mechanics of composite materials, the fabric stress has been derived in the X-direction (see Fig. 1), as shown in Eq. 4.

$$T(\alpha) = \sum_{i=1}^{n} \sigma^f \cos^2 \beta_i V_f \chi(\beta_i) \qquad (4)$$

where $T(\alpha)$ is the fabric stress in a given test direction (α), V_f is the fibre volume fraction, and $\chi(\beta_i)$ be a frequency of ith bin of a histogram, representing the distribution as a function of the measured or initial fibre orientation angle (β_i) between fibre and test directions of the fabric.

Based on Eq. 1, fibre stress is dependent upon fibre strain (ε_f) and the relationship between fibre and fabric strains has been obtained assuming the material to be orthotropic in nature [21].

$$\varepsilon_f = \cos^2 \beta_i \bar{\varepsilon} - v\bar{\varepsilon} \sin^2 \beta_i + \sin \beta_i \cos \beta_i \gamma \qquad (5)$$
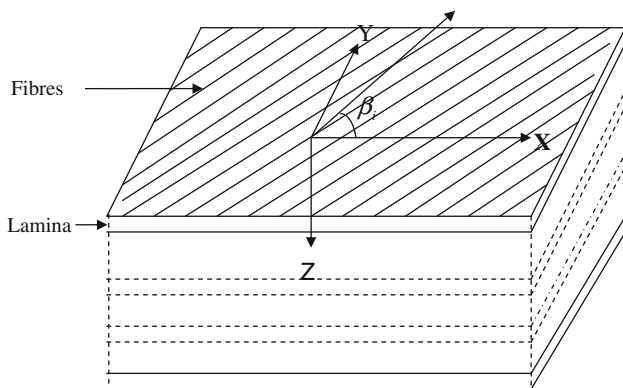

Fig. 1 Nonwoven simulated as a *laminate*

where $\bar{\varepsilon}$ is the fabric strain and γ is the shear strain.

Thus, the stress–strain behaviour of a nonwoven structure can be predicted using Eqs. 1, 4 and 5.

Rawal et al. [19] tensile model of nonwoven structures

In our previous research work, a mesodomain was considered consisting of a fibre connected with the bonds at its ends and the mesodomain is a constituent of a macroscopic volume, V, such that it has a unit cross-sectional area and volume, dV [19, 22]. Subsequently, the number of contacts or bonds in the volume dV was calculated and the fabric stress was calculated by considering the effect of fibre re-orientation, as shown below [19].

$$T(\alpha) = \sum_{j=1}^{n} m K_\alpha(\beta_f) \cos \beta_{fj} \chi(\beta_{fj}) \sigma^f(\beta_f, \bar{\varepsilon}) \qquad (6)$$

$$K_\alpha(\beta_f) = \int_{-\pi/2-\alpha}^{\pi/2-\alpha} |\cos(\beta_f)| \chi(\beta_f) d\beta_f \qquad (7)$$

$$\beta_f = \cos^{-1} \left[\frac{(1 + \bar{\varepsilon})}{\sqrt{(1 + \bar{\varepsilon})^2 + \tan^2 \beta_i (1 - v\bar{\varepsilon})^2}} \right] \qquad (8)$$

where m is the mass per unit area of the nonwoven, β_i is the measured or initial fibre orientation angle, $\chi(\beta_{fj})$ be a frequency of j-th bin of a histogram, representing the distribution as a function of the final fibre orientation angle (β_f) at defined level of fabric strain ($\bar{\varepsilon}$) and K_α is the directional parameter.

It must be noted that mass per unit area of the fabric is also being updated with the applied strain. This can be simply considered by taking the product of initial mass per unit area at zero strain and directional parameter, which is being updated at various levels of strain. Since, we have considered the model to be two-dimensional (2D) in nature, the changes in the thickness have been ignored during the application of strain.

As mentioned earlier, the fibre stress (σ^f) is a function of fibre strain (ε_f), and we have used the relationship between fibre and fabric strains as illustrated in Eq. 3.

Furthermore, in the case of thermally bonded nonwovens the tensile strength has also been determined through the maximum pull-out stress (P_{max}) required for breaking the fibre–bond interface [19].

$$P_{max} = \text{Int}\left(\frac{2V_f}{\pi D^2} K_\alpha\right) \frac{\tau_b w_b}{\rho} \tanh \rho \bar{b}_b \qquad (9)$$

$$\rho = \sqrt{\frac{G_b w_b}{E_f \pi r_f^2 t_b}} \qquad (10)$$

$$w_b = \sqrt{(\bar{b}_b - D)^2 + D^2} \tag{11}$$

$$\bar{b}_b = D \left\{ \int_{-\pi/2-\alpha+\beta_f'}^{\pi/2-\alpha+\beta_f''} \frac{1}{|\sin(\beta_f)|} \chi(\beta_f) d\beta_f \right\} \tag{12}$$

Also $\quad \beta_f'' > \beta_f > \beta_f' \tag{13}$

where $\quad \beta_f'' = \pi - \sin^{-1}\left(\frac{D}{l_f}\right) \tag{14}$

and $\quad \beta_f' = \sin^{-1}\left(\frac{D}{l_f}\right) \tag{15}$

where w_b is the mean width of the bond, r_f is the radius of the fibre, D is the diameter of the fibre, $t_b(\approx 0.8 r_f)$ is the thickness of the bond [20], E_f is the fibre modulus, l_f is the average fibre length, V_f is the fibre volume fraction and G_b, τ_b are the shear modulus and shear strength of bond formed between the fibres, respectively.

Here, Int( ) is the integer function in Eq. 9, which omits the fractional part of the result as to indicate the discrete bonds.

It must be noted fibre and bond parameters are given in our previous articles [19, 22] and the shear modulus and shear strength of bond are considered to be 0.1 GPa and 10 MPa, respectively [13].

The reader is referred to our previous article [19] for the obtaining the details of abovementioned equations.

Experimental

The reported study is based on two thermally bonded nonwoven structures, produced and supplied by the company, i.e. Libeltex in the previous research work, and labelled here as TB1 and TB2 [22]. The main difference between the thermally bonded nonwovens TB1 and TB2 is that relatively finer fibres have been used in TB1 in comparison to TB2. Some of the important fabric and constituent fibre properties are already reported in our previous article [19]. Moreover, the validation of initial tensile model has also been extended to spunbonded nonwoven structure. This structure has been obtained from the company (Colbond), and the constituent filaments are bicomponent (sheath-core) type having polyamide-6 and polyester as sheath and core components, respectively. Figure 2 illustrates the stress–strain curve of bicomponent filament obtained from spunbonded nonwoven structure. In general, a third degree polynomial is fitted to simulate the stress–strain behaviour of fibre/filament in a nonwoven structure. The mass per unit area and thickness of the spunbonded fabric are 100 g/m² and 0.50 mm, respectively. The thickness was measured at a pressure of
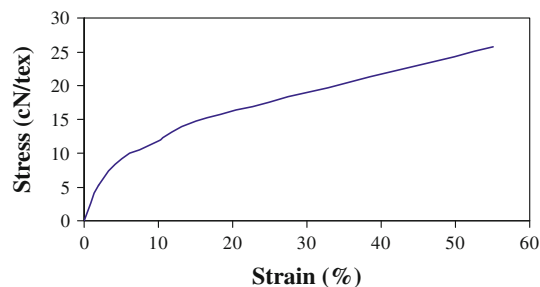

Fig. 2 Stress–strain curve of bicomponent filament obtained from spunbonded nonwoven

Table 1 Properties of constituent filament used in the production of spunbonded (SB) structure

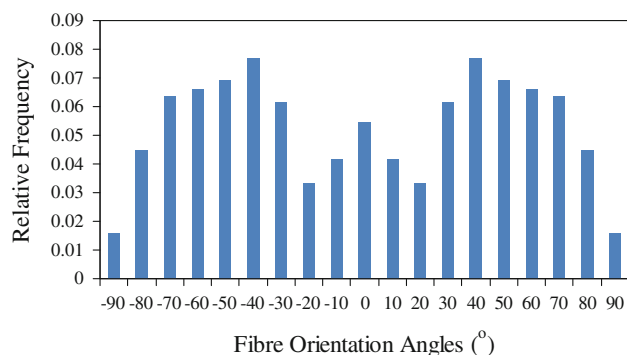| Type of fibres	Polyester (core)	Polyamide-6 (sheath)
Volume (%)	74	26
Linear density (dtex)		14.5
Diameter (μm)		37.5

Fig. 3 In-plane fibre orientation distribution of spunbonded nonwoven
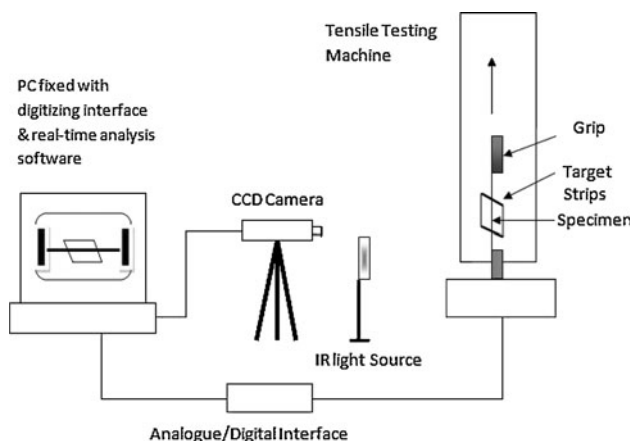

Fig. 4 Schematic view of videoextensometer and tensile testing stage

Table 2 Shear strain values of thermally bonded nonwoven structures

Longitudinal strain (%)	Test direction (°)									
	0		22.5		45		67.5		90	
	TB1	TB2	TB1	TB2	TB1	TB2	TB1	TB2	TB1	TB2
1	0.01	0	0.01	0	0.01	0	0.01	0.01	0.01	0.01
2	0.01	0.01	0.01	0	0.02	0.01	0.01	0.01	0.01	0.01
3	0.01	0.02	0.03	0.01	0.03	0.01	0.02	0.01	0.01	0.01
4	0.02	0.02	0.04	0.01	0.05	0.01	0.02	0.01	0.01	0.01
5	0.02	0.03	0.04	0.02	0.06	0.01	0.02	0.01	0.01	0.01

20.68 kPa using the ASTM D5729-95. The important constituent filament parameters are given in Table 1. The fibre orientation was also measured by digitally capturing and analysing the images using optical microscope and LEICA QWIN software. The histograms of the relative frequency of fibres for 10° orientation angle interval with respect to the machine direction were computed to characterise the orientation distribution. Figure 3 shows the histogram of relative frequency of fibres that have been used in the production of spunbonded nonwoven (0° indicating the machine direction). Nonwoven strips of 30 × 5 cm were tested on an Instron tensile testing machine under uniaxial loading at a strain rate of 10 mm/min with the width and gauge length of 50 and 200 mm, respectively. Furthermore, Poisson's ratios of various nonwoven structures were obtained at different strain levels using Messphysik® videoextensometer. Here, a charge couple device (CCD) camera was mounted perpendicular to the plane of tensile testing machine and four markers/targets have been placed on the nonwoven sample such that a square of dimensions 4 × 4 cm² is formed between them. Subsequently, the infrared was used as source of illumination and a computer is attached to the videoextensometer to record the changes in width and length of nonwoven sample. It is worth mentioning that the software used for videoextensometer works on the principle of evaluation of the grey contrast between the specimen surface and the markers. Figure 4 shows the schematic view of videoextensometer and tensile testing stage. The shear strain specifically at lower levels of longitudinal strains was also determined similar to the technique employed by Bais-Singh and Goswami [7]. Tables 2 and 3 show the shear strain values at various longitudinal strains for thermally bonded and spunbonded nonwoven structures.

Results and discussion

Figure 5 illustrates the Poisson's ratio values at lower levels of strain for thermally bonded nonwovens. It is observed that Poisson's ratio is relatively higher in the

Table 3 Shear strain values of spunbonded nonwoven structure

Longitudinal strain (%)	SB
1	0
2	0.01
3	0.01
4	0.01
5	0.02
6	0.02
7	0.02
8	0.02
9	0.03
10	0.04

machine direction (0°) due to the fact that relatively more number of fibres are orientated in the region of machine direction. Similarly, Fig. 6 shows the Poisson's ratio values at various levels of strain for a spunbonded nonwoven structure. In general, there is a distinct difference between the curves of thermally bonded and spunbonded nonwovens specifically in the machine direction. The thermally bonded curve sharply increases up to 2–3% of strain and subsequently characterised by a *plateau* whereas the spunbonded continues to increase even at higher levels of strain ($\approx 10\%$). This is mainly due to difference in the inherent structural characteristics of spunbonded and thermally bonded nonwoven structures. In this study, the fibre orientation in spunbonded nonwoven is found to be almost random in nature (see Fig. 3) whereas the fibre alignment in thermally bonded nonwoven structures is *preferential* type [19]. On applying the tensile load, limited fibre re-orientation occurs in a *preferential* type of structure whereas the fibre re-orientation continues in a random structure such as spunbonded nonwoven. To further elucidate the influence of the Poisson's ratio on fibre re-orientation, an additional *virtual* experiment was carried out based on an analysis of idealised nonwoven using Eq. 8. Figure 7 shows the relationship between fibre re-orientation and Poisson's ratio at a longitudinal strain of 20%. It is demonstrated in a *virtual* experiment that fibres lying other than the machine and cross-machine directions

Fig. 5 Relationship between Poisson's ratio and longitudinal strain in nonwovens **a** TB1 and **b** TB2 in various test directions
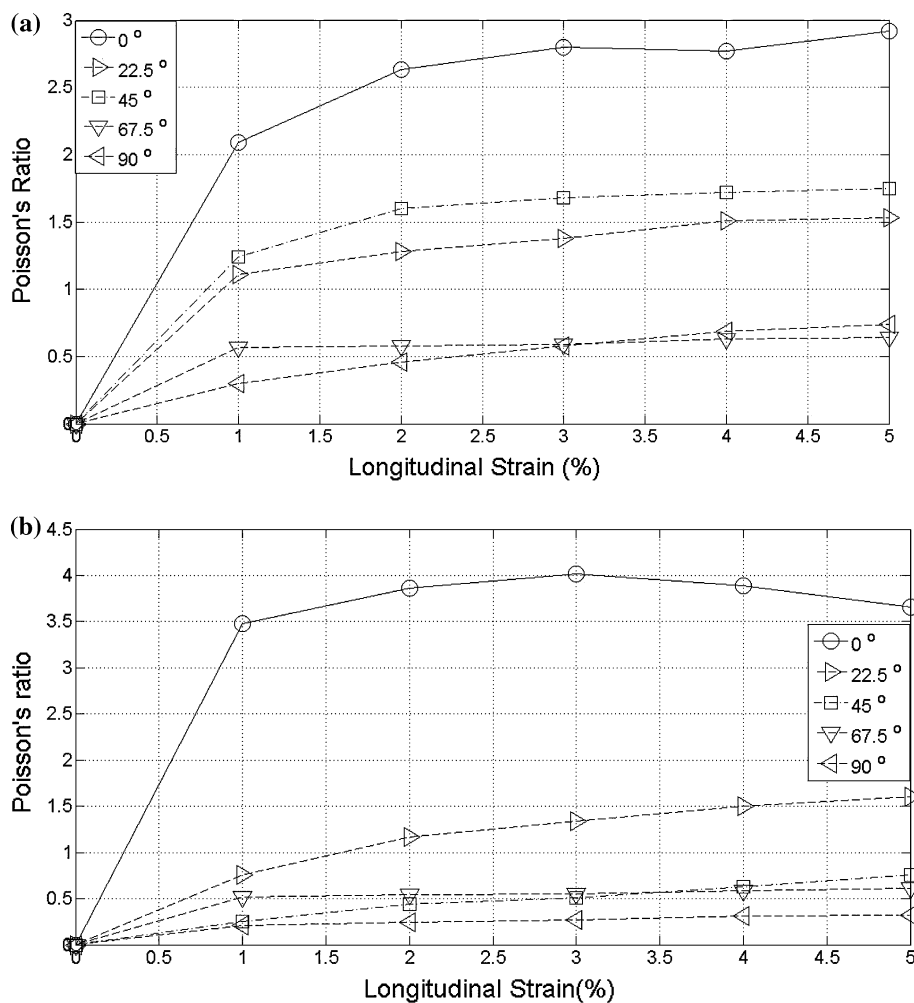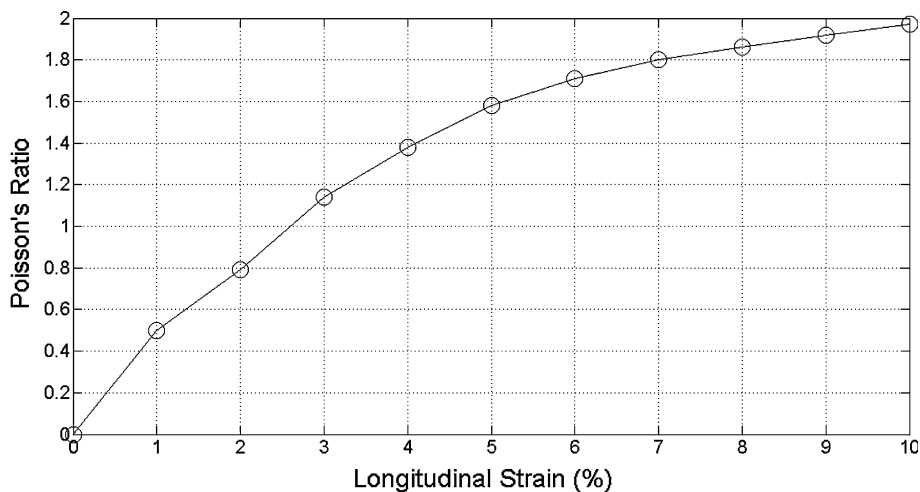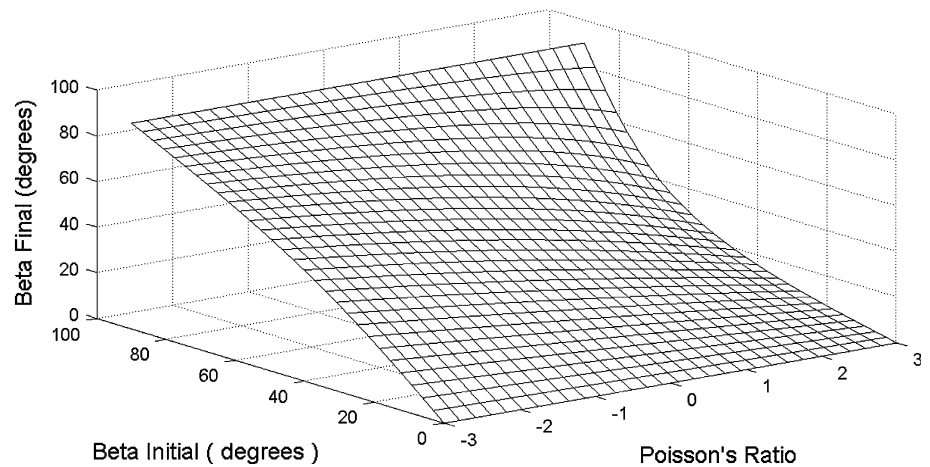

Fig. 6 Relationship between Poisson's ratio and longitudinal strain in a spunbonded nonwoven structure

continue to move against the test direction in a nonwoven characterised by negative Poisson's ratio. On the other hand, the fibre re-orientation towards the loading direction occurs *non-linearly* in a nonwoven having positive Poisson's ratio indicating that the relative movement of fibres

orientated in the region of cross-machine direction (90°) is quite minimal towards the loading direction (0°). Nevertheless, significant re-orientation occurs in the fibres initially orientated between 40 and 70° with respect to the machine direction.

Comparison between experimental and theoretical results

A comparison is made between the experimental and theoretical stress–strain curves. These theoretical results have been obtained from the most popular analytical models available in the literature in addition to our model [6, 7, 19]. It must be noted that the fabric stress obtained from Hearle's model is generally expressed in N/tex and has been converted into MPa. This has been considered by taking the product of fabric stress (N/tex) and fabric density (kg/m^3) and hence, yielded the expression in MPa. Figures 8 and 9 illustrate a comparison between the theoretical and experimental stress–strain curves of thermally bonded nonwovens in various test directions. Similarly, Fig. 10 shows a comparison between the predicted and experimental stress–strain curves of a spunbonded nonwoven specifically in the machine direction (0° test direction). The following observations can be deduced from the above figures.

- The experimental stress–strain curves specifically in the 0° test directions are nonlinear in nature. Since, the fibres/filaments oriented other than the machine direction tend to re-orientate without bearing the load results in a *dwell period* that may cause nonlinearity in the stress–strain curve [23].
- A good agreement has been obtained between the theoretical and experimental results of stress–strain curves specifically, in the case of TB1. This is primarily due to the fact that directional parameter (as shown in Eq. 7) has been incorporated in our model that reflects the projection of average fibre length between the bonds on the test direction at various levels of strain. This average fibre length between the bonds is updated at various levels of strain by means of fibre re-orientation as computed in Eq. 8. Table 4
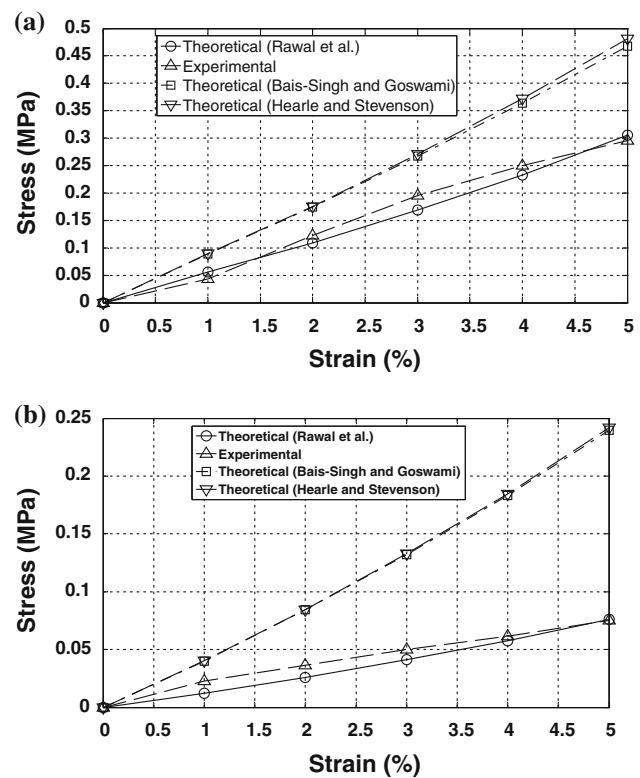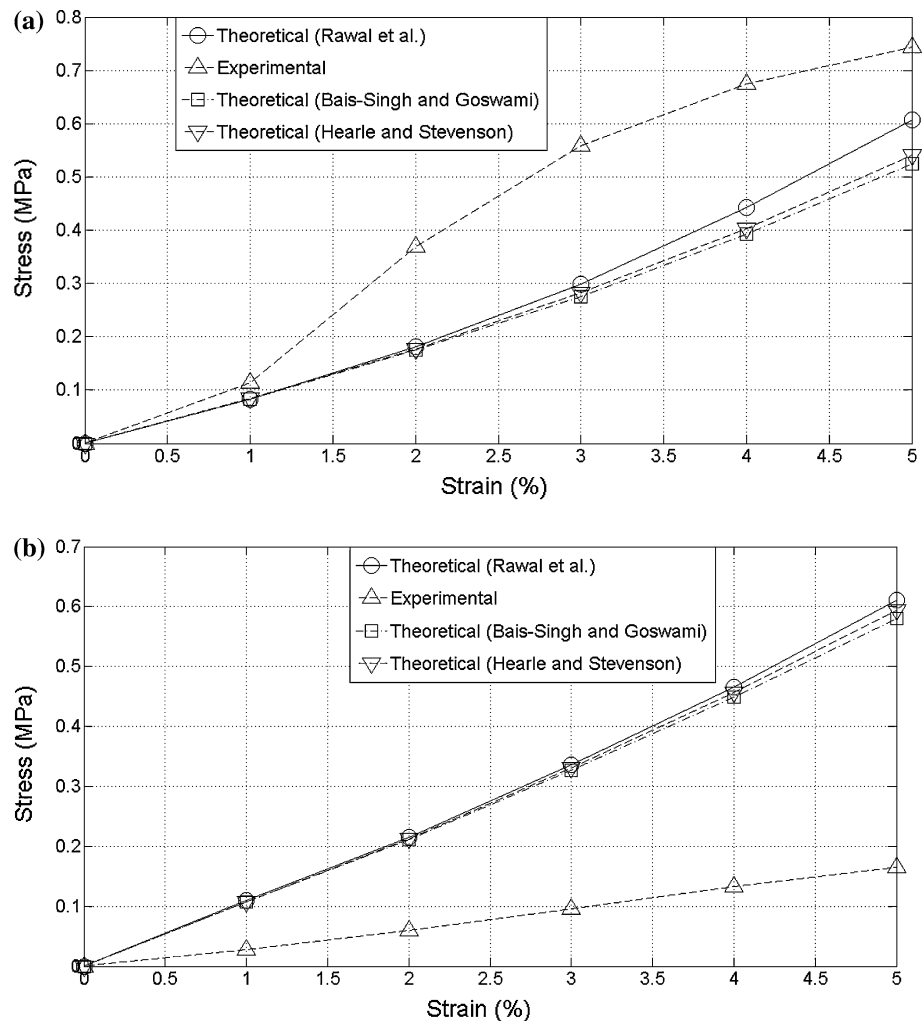

Fig. 8 Comparison between theoretical and experimental stress–strain curves of thermally bonded nonwoven TB1 in **a** 22.5° and **b** 67.5° test direction

shows the values of directional parameter values of thermally bonded nonwovens in various test directions. However, in the case of TB2 theoretical model overestimated the experimental stress–strain results, specifically in 22.5° test direction. This may be due to the experimental errors involved in determination of fibre orientation distribution specifically for a nonwoven structure produced from coarser fibres. Since, there are structural inherent nonuniformities present in

Fig. 9 Comparison between theoretical and experimental stress–strain curves of thermally bonded nonwoven TB2 in **a** 0° and **b** 22.5° test direction

a typical coarser fibre-based nonwoven fabric [22]. Similar observations have been made in the case of spunbonded nonwoven structure produced from coarser fibres. Furthermore, the effect of fibre crimp needs to be accounted as it has a considerable effect in determining the initial tensile behaviour of nonwoven structures [24].

The tensile strength of thermally bonded nonwovens has also been predicted based on the *maximum pull-out stress* (shown in Eq. 9), and subsequently, a comparison is made between theoretical and experimental tensile strengths (see Fig. 11). It has been demonstrated there is a good agreement between theoretical and experimental tensile strengths specifically for thermally bonded nonwoven, i.e. TB1. However, in the case of TB2 there is a large over-estimation of tensile strength made in test directions other than 0°. As mentioned earlier, this is due to the presence of structural *in-homogeneities* (fibre orientation distribution, porosity, pore size distribution, etc.) present in a nonwoven structure produced from coarser fibres. The occurrence of
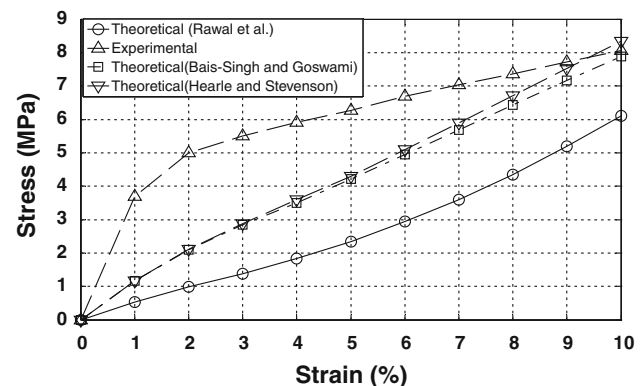

Fig. 10 Comparison between theoretical and experimental stress–strain curves of spunbonded in 0° test direction

in-homogeneities in coarser fibre-based nonwoven is primarily due to the presence of less number of fibres, in comparison to the finer fibres present in a nonwoven structure of same mass per unit area.

Table 4 Directional parameter values of thermally bonded nonwoven structures

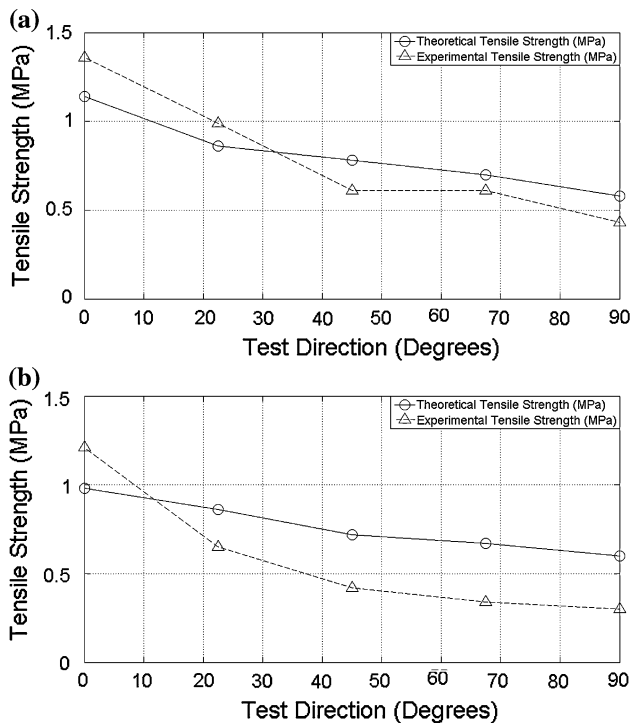| Longitudinal strain (%)	Test direction (°)									
	0		22.5		45		67.5		90	
	TB1	TB2	TB1	TB2	TB1	TB2	TB1	TB2	TB1	TB2
1	0.81	0.77	0.76	0.73	0.65	0.65	0.52	0.54	0.42	0.48
2	0.82	0.78	0.76	0.73	0.65	0.65	0.52	0.54	0.43	0.49
3	0.83	0.79	0.76	0.74	0.65	0.65	0.52	0.55	0.43	0.49
4	0.84	0.80	0.77	0.74	0.65	0.65	0.52	0.55	0.43	0.49
5	0.85	0.80	0.77	0.74	0.65	0.65	0.52	0.55	0.43	0.50

Fig. 11 Comparison between theoretical and experimental tensile strengths of thermally bonded nonwovens **a** TB1 and **b** TB2 in various test directions

Conclusions

A comparison is made between the theoretical and experimental stress–strain curves of thermally bonded and spunbonded nonwoven structures. The theoretical findings have been obtained from the most popular analytical models of stress–strain behaviour of nonwovens available in the literature in addition to our modified tensile model [6, 7, 19]. The directional parameter included in our model is found to be useful in predicting the tensile behaviour of nonwovens specifically in test directions other than the machine direction. In general, a close agreement was found between the predicted and the experimental stress–strain curves specifically at lower level of strains. An accurate

measurement of fibre orientation distribution is a pre-requisite to predict the stress–strain behaviour of nonwoven structures. Furthermore, fibre re-orientation in random and anisotropic (preferential) nonwoven structures is found to be significantly different as revealed between the relationship of Poisson's ratio and longitudinal strain. It was established that fibre pull-out can be considered as the failure criterion for thermally bonded nonwoven structures as the tensile strength of thermally bonded nonwoven structures matched well specifically in the machine direction.

References

1. Lukić S, Jovanić P (2004) Mater Lett 58:439
2. Patnaik A, Tejyan S, Rawal A (accepted) Soil erosion behaviour of needlepunched nonwoven reinforced composites. Res J Text Appar
3. Engelmayr GC, Sacks MS (2006) J Biomech Eng 128:610
4. Backer S, Petterson DR (1960) Text Res J 30:704
5. Hearle JWS, Stevenson PJ (1963) Text Res J 33:877
6. Hearle JWS, Stevenson PJ (1964) Text Res J 34:181
7. Bais-Singh S, Goswami BC (1995) J Text Inst 86:271
8. Kim HS (2004) Fibers Polym 5:139
9. van Wyk CM (1946) J Text Inst 37:T285
10. Komori T, Makishima K (1977) Text Res J 47:13
11. Komori T, Makishima K (1978) Text Res J 48:309
12. Pan N (1993) Text Res J 63:336
13. Pan N, Chen J, Seo M, Backer S (1997) Text Res J 67:907
14. Mueller DH, Kochmann M (2004) Int Nonwovens J 13:56
15. Limem S, Warner SB (2005) Text Res J 75:63
16. Hou X, Acar M, Silberschmidt VV (2009) Comput Mater Sci 46:700
17. Demirci E, Acar M, Pourdeyhimi, B, Silberschmidt VV (in press) Comput Mater Sci. doi:10.1016/j.commatsci02:039
18. Hou X, Acar M, Silberschmidt VV (in press) Comput Mater Sci. doi:10.1016/j.commatsci.2010.03.009
19. Rawal A, Priyadarshi A, Lomov SV, Ngo T, Verpoest I, Vankerrebrouck J (2010) J Mater Sci 45:2274. doi:10.1007/s10853-009-4152-x
20. Pan N (1993) J Text Inst 84:472

21. Jones RM (1975) Mechanics of composite materials. McGraw-Hill, New York
22. Rawal A, Lomov SV, Ngo T, Verpoest I, Vankerrebrouck J (2007) Text Res J 77:417
23. Rawal A, Lomov SV, Verpoest I (2008) J Text Inst 99:235
24. Rawal A (2006) J Ind Text 36:133